

Cr(III), Mn(II), Co(II), Ni(II) and Cu(II) complexes of 7-((1H-benzo[d]imidazol-2-yl)diazetyl)-5-nitroquinolin-8-ol. synthesis, thermal, spectral, electrical measurements, molecular modeling and biological activity

Mohamed Gaber ^{a,*}, Nadia El-Wakiel ^a, Osama M. Hemeda ^b

^a Chemistry Department, Faculty of Science, Tanta University, Tanta, 31527, Egypt

^b Physics Department, Faculty of Science, Tanta University, Tanta, 31527, Egypt



ARTICLE INFO

Article history:

Received 4 September 2018

Received in revised form

22 November 2018

Accepted 4 December 2018

Available online 5 December 2018

Keywords:

Azodye complexes

TGA

Modeling

Antimicrobial

Conductivity

ABSTRACT

The titled new azo-compound namely, 7-((1H-benzo [d]imidazol-2-yl) diazenyl)-5-nitroquinolin-8-ol, and its Cr(III), Mn(II), Co(II), Ni(II) and Cu(II) complexes have been designed and prepared. These compounds were characterized by spectral and analytical techniques. The IR spectral data suggested that the free compound behaves as dibasic tridentate via deprotonated OH, NH and N atom of azo group. Cr(III) and Ni(II) complexes have octahedral, Mn(II) and Cu(II) complexes have square planar while Co(II) complex has tetrahedral geometry. The molecular parameters were calculated to secure the geometry of the complexes. The thermal studies have been undertaken as an additional information to confirm the structure of the studied complexes. The kinetic and thermodynamic parameters of the thermal decomposition steps were evaluated using three mechanistic equations at different heating rates (5–15 °C/min). The activities of the ligand and its complexes have been tested as antimicrobial strains. All complexes have higher biological activity than free ligand. The solid state electrical conductivity of the metal complexes was measured.

© 2018 Elsevier B.V. All rights reserved.

1. Introduction

An azodye is a particular class of synthetic organic dye that possess a number of chemical features that make the molecule as sensitive to its environment [1–3]. Metal-based azocompounds have attracted increasing attention because of their uses in many important areas such as in dye industry as analytical reagents for the metal ions determination [4–6] as well as in supramolecular chemistry [7] in addition to widespread dyeing characters [8,9], photoelectronics and sensitizers in photocatalytic reactions [10–12] as well as in optical information storage [13–15]. Furthermore, azo-compounds and their complexes are known to be involved in a wide range of potential medical applications. This class of compound exhibited a broad range of biological activities such as antibacterial, antitumor, antioxidant as well as anticancer

properties [16–26]. Many azocompound complexes were reported and the results indicated that their biological activities are more active than free azodyes. This is due to chelation formation which decreases the polarity of the metal ions. Azo-compounds based on 8-hydroxyquinoline derivatives play a central role as chelating agents for a large number of metal ions [27,28] as well as Hg²⁺ selective chemosensors selective solid phase extraction of trace lead from environmental samples [1,6]. Also, some 8-hydroxyquinoline and azo derivatives found numerous applications in analytical chemistry as chromophoric and metallochromic indicators [29,30].

Our aim was to take into account all the previously mentioned characters of azo compounds and synthesized new metal complexes derived from azodye to develop some novel bioactive metal complexes of ONN donor azodye ligand. Thus, we were motivated to undertake a systematic study for elucidation of the structures of the investigated a new azodye and its Cr(III), Mn(II), Co(II), Ni(II) and Cu(II) complexes using different spectral and analytical techniques. The theoretical calculations have been done to confirm the structures of the compounds under investigation. The electrical

* Corresponding author.

E-mail addresses: mabuelazm@science.tanta.edu.eg, mabuelazm@hotmail.com (M. Gaber).

conductance of the azodye and its metal complexes was measured at different temperatures using different frequency values to define the electrical conduction mechanism of the studied samples.

2. Experimental

2.1. Materials

All compounds used in the present study were of pure analytical available from BDH, Aldrich or Sigma. They include 2-aminobenzimidazole (Sigma-Aldrich, 97%), 5-nitro-8-Hydroxyquinoline (Sigma-Aldrich, 95%), HCl(35%), NaNO₂(Merck, 99%), CrCl₃.6H₂O, MnCl₂.4H₂O, CoCl₂.6H₂O, NiCl₂.4H₂O and CuCl₂.2H₂O].

2.2. Synthesis of the ligand

The azo dye ligand H₂L (Fig. 1) was prepared by dissolving 1.33 gm (0.01 mol) of 2-aminobenzimidazole in 25 ml of distilled water containing 2.5 ml of conc. HCl (35%). The resulting solution was then cooled under stirring to 0 °C. A cold solution containing 0.69 gm (0.01 mol) of sodium nitrite in 25 ml of distilled water, was drop wisely added to the previous solution to form the diazonium chloride. This solution was then added to a solution containing 1.90 ml of 5-nitro-8-hydroxyquinoline (0.01 mol) dissolved in 10 ml of water containing 0.4 gm (0.01 mol) of NaOH. The yellow dye, which separated out, was kept in an ice bath under stirring for 30 min. The precipitate was then filtered off, washed by distilled water, and finally air dried (yield: 75%). Scheme 1 represents the synthetic procedure of the azodye ligand.

2.3. Synthesis of metal complexes

Metal complexes have been prepared by mixing appropriate amounts of the H₂L ligand (0.334 gm, 1 mmol) in a DMF/MeOH mixture (20% V/V) with (1 mmol) of the hydrated metal chlorides [CrCl₃.6H₂O, MnCl₂.4H₂O, CoCl₂.6H₂O, NiCl₂.4H₂O and CuCl₂.2H₂O] in absolute methanol. The resulting solutions were then refluxed with stirring for 4 h; the solid complexes which separated out on hot have been collected by filtration and dried in vacuum desicator over anhydrous CaCl₂.

2.4. Instrumentation

The elemental analyses were performed, at the micro analytical center, Cairo University, on Perkin-Elmer 2400 CHN Elemental analyzer. Metal content was estimated using inductive coupled plasma (ICP) Perkin Elmer/Optima 7000 DV at central laboratory, Tanta University. Molar conductivities were determined in DMF (10^{-3} M) at room temperature (25 °C) with a 523 conductivity bridge. The Infrared spectra (4000–400 cm⁻¹) for KBr discs were performed with a JASCO FT/IR-4100 spectrophotometer. Standard

electron impact mass spectra (EI) were recorded using a Finnigan MAT 8222 Spectrometer at 70 eV at micro analytical unit of Cairo University. The NMR measurements were carried out in DMSO-d₆ using a Varian Mercury Oxford NMR 300 Hz at room temperature by using TMS as an external standard. The electronic spectra were measured as Nujol mull [31] using a Shimadzu UV–Vis 240 spectrophotometer. The corrected molar magnetic susceptibilities have been determined at 25 °C using magnetic susceptibility balance (Johnson Mtthey) 436 Devon Park Drive employing the Gouy's method and the diamagnetic corrections were made by using Pascal's constants [32]. The thermogravimetric analyses (TG) of the solid samples have been performed within the temperature range 25–800 °C using the Shimadzu TG-50 thermogravimetric analyzer at different heating rates (5–15 °C/min.) under nitrogen atmosphere.

2.5. Molecular modeling studies

Several attempts to grow appropriate crystals for X-ray crystallography were unsuccessful. The use of theoretical parameters help to characterize the molecular structure of the studied complexes. An attempt to gain a better insight on the molecular structure of metal complexes, geometric optimization and conformational analysis has been performed by the use of MM + force field as implemented in hyperchem 8.0 [33]. Molecular orbital geometry optimization allows a quantitative discussion not only of the geometry but also the ground electronic properties of the investigated complexes. Geometric and electronic structures of the ligands and their metal complexes were calculated by the optimization of their bond lengths, bond angles and dihedral angles.

2.6. Antimicrobial studies

The antimicrobial activities of the newly synthesized azo-compound and its Mn(II), Co(II), Ni(II) and Cu(II) complexes have been screened against *C. albicans*, *A. niger* as well as *E. coli* (Gram-negative bacteria) and *S. aureus* (Gram-positive bacteria). The standard drugs, Fluconazole (antifungal) and Penicillin (antibacterial), were also tested. The in vitro antimicrobial activities of the newly prepared compounds were evaluated using the agar diffusion technique [34]. 1 mg/ml solution in dimethyl formamide was used. The bacteria and fungi used were maintained on nutrient agar media and CzapeksDox agar medium, respectively. DMF showed no inhibition zones. The agar media were inoculated with different test microorganism. After 24 h. of incubation at 30 °C for bacteria and 48 h of incubation at 28 °C for fungi, the diameter of inhibition zone (mm) was measured. Every treatment was replated three times. The biological activities of the azodye ligand and its complexes were screened for their antifungal activity (*C. albicans* and *A. niger*) and antibacterial activity (*E. coli* and *S. aureus*). The standard drugs, Fluconazole (antifungal) and Penicillin (antibacterial), were also tested at the same experimental conditions.

2.7. Electrical conductivity

The electrical resistivities were measured for free compound and its metal complexes in the form of discs (diameter 1.5×10^{-2} m and of thickness 2×10^{-3} m). The measurements were carried out in air within the temperature range 298–525 K using RLC bridge. A good contact of the electrodes with the surfaces of the disc was obtained by painting carefully these surfaces using a silver paste. The temperature was measured using a Ni–Cr thermocouple placed closed to the sample. The large particle size of Ag and the very fast dry of the Ag past make it impossible to be difused in the sample surface.

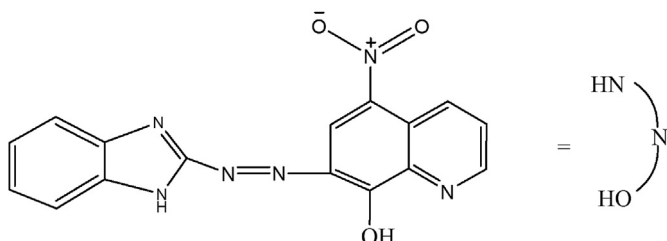
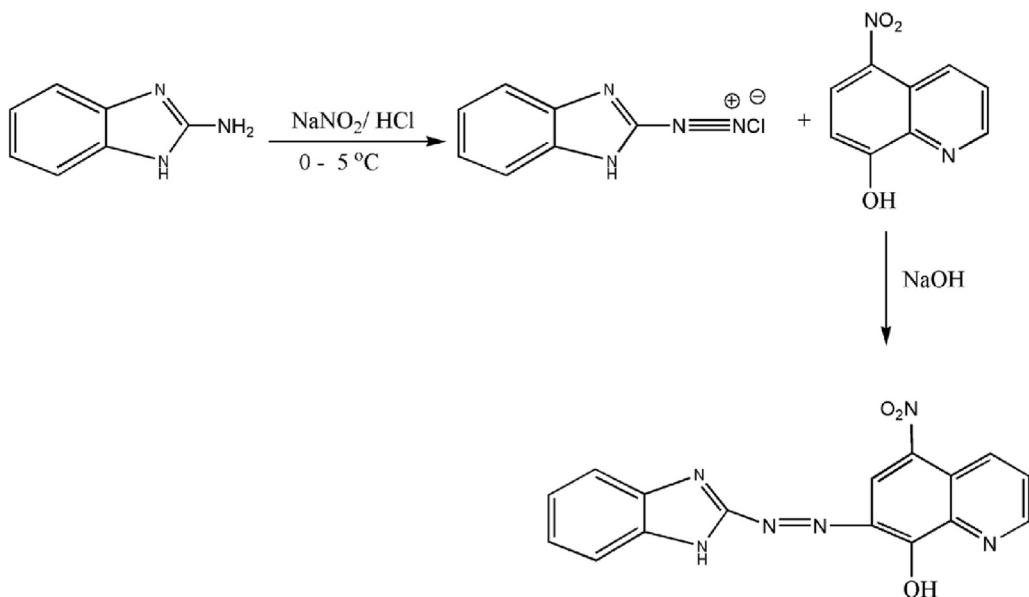


Fig. 1. Proposed structure of azodye ligand (H₂L).



Scheme 1. The synthetic procedure of the azodye ligand, H_2L .

3. Results and discussion

3.1. Study of ligand

The IR spectrum of the free azodye (Fig S1) exhibited bands at 1633 and 1600 cm^{-1} due to the azomethine group of the quinoline and benzimidazole rings while $\nu(\text{N}=\text{N})$ appeared at 1419 cm^{-1} . The band appeared at 3247 cm^{-1} is due to N–H group. For the free ligand, the C–O band is observed at 1321 cm^{-1} . The mass spectrum of the ligand is shown in Fig S2. The mass spectrum of the ligand showed a molecular ion peak at m/z 334 which is equivalent to the molecular weight of the ligand. The peaks at m/z = 273, 190, 165, 132 and 105 are due to fragments shown in Scheme S1. The most important fragments are that appeared at 165 and 105 which confirmed the formation of the azo compound. ^1H NMR spectrum of the ligand (Fig. S3) exhibited a signal at 8.98 ppm assigned to the OH group of 8-hydroxyquinoline ring. This downfield shift is due to intramolecular hydrogen bonding between OH and N-atom of the quinoline ring. The signal assigned to NH-imino protons appeared at 7.91 ppm. The signals within the regions of 9.20–9.13 and 8.53–7.83 ppm assigned to all the aromatic protons of the quinoline ring. The aromatic protons of benzimidazole ring appear as multi signals in the region 7.726–7.11 ppm.

3.2. Study of complexes

All the solid metal chelates are colored, stable towards air and moisture, and soluble in DMF. The analytical results of the complexes are consistent with the proposed molecular formulae and confirm the formation of 1:1 (M: L) complexes Table 1. The molar conductance of metal complexes was measured for 10^{-3} M solution in DMF at room temperature (Table 1). The low molar conductance values of the metal complexes ($A_M = 8\text{--}2.23\text{ } \Omega^{-1}\text{ cm}^2\text{ mol}^{-1}$) confirm their non electrolytic nature [35].

3.2.1. IR spectra

Verification of the structure of metal complexes can be easily achieved by comparing the IR spectrum of the free ligand with its metal complexes (Table 2), (Fig. S1).

It was found that the bands due to the azomethine group of the

quinolone (1633 cm^{-1}) and benzimidazole (1600 cm^{-1}) rings [36] appeared almost at the same position in the spectra of all complexes suggesting that the N-atom of these groups is not participated on chelation. On the other hand, the ligand band $\nu(\text{N}=\text{N})$ appearing at 1419 cm^{-1} is shifted to higher or lower wavenumbers by $42\text{--}46\text{ cm}^{-1}$ in the spectra of complexes suggesting its involvement in coordination sphere [37]. The spectrum of the free ligand shows a band at 3247 cm^{-1} which allocated to $(\nu\text{NH})\text{Bz}$ [36]. The disappearance of this band for all complexes indicated the deprotonated N–H participate in chelation. The C–O band of the free ligand (1321 cm^{-1}) [38] was shifted to higher values by $22\text{--}39\text{ cm}^{-1}$ indicating the participation of the oxygen atom of phenolic group in complex formation through deprotonation [22,39]. New bands appeared within the ranges $577\text{--}549$ and $460\text{--}439\text{ cm}^{-1}$ due to $\nu(\text{M}-\text{O})$ and $\nu(\text{M}-\text{N})$ bands, respectively, supporting the participation of the oxygen atom of OH group and N atom of azo group in complex formation [22,40–42]. The appearance of a broad band within $3458\text{--}3430\text{ cm}^{-1}$ range in the spectra of hydrated complexes are assigned to $\nu(\text{OH})$ of water molecule [43]. According to IR spectral data, it was concluded that the ligand behaves as dibasic tridentate ligand.

3.2.2. Thermal behavior of metal complexes

The thermal behavior of the azodye ligand and its metal complexes was characterized on the basis of TG technique. Thermoanalytical data of the complexes are given in Table 3. The TG thermograms of all compounds are represented in Fig. S4.

Cr(III) complex decomposed within four successive steps. The first step occurred within the range $29\text{--}100\text{ }^\circ\text{C}$ correspond to the loss of coordinated methanol molecule. The second step of decomposition appeared within the range $100\text{--}179\text{ }^\circ\text{C}$ due to the loss of coordinated water molecule. The third step occurred within the range $179\text{--}267\text{ }^\circ\text{C}$ assigned to the loss of coordinated chloride ion. The last step of decomposition appeared as sharp peak within the range $312\text{--}400\text{ }^\circ\text{C}$ which due to the decomposition organic ligand leaving the metal oxide as final product. Mn(II) and Cu(II) complexes decomposed within two successive steps. The first step occurred within the ranges $28\text{--}142$ and $28\text{--}176\text{ }^\circ\text{C}$ for Mn(II) and Cu(II) complexes, respectively. These steps correspond to the loss of one coordinated water molecule. The second step of decomposition

Table 1The analytical and physical data of the ligand (H_2L) and its metal complexes.

formulae	Color/ Λ_m^a	Yield/%	Elemental analysis/%			Mol. wt
			Calc./found	C	H	
H_2L $C_{16}H_{10}N_6O_3$	yellow	75	57.49/57.54	3.02/3.10	—	334.29/334*
$[CrClMeOH\ H_2O]$	Orange/2.50	85	43.46/43.89	3.00/2.59	11.07/11.36 13.26 ^b	469.78
$C_{17}H_{14}CrClN_6O_6$					13.56/14.04 12.74 ^b	405.23
$[MnL\ H_2O]$	Dark brown/3.19	70	47.42/46.82	2.49/2.64	13.24/13.10 12.58 ^b	445.25
$C_{16}H_{10}MnN_6O_4$					12.30/12.96 11.69 ^b	477
$[CoLH_2O]\ 2H_2O$	Orange/2.23	75	43.16/43.62	3.17/3.13	15.36/14.94 15.13 ^b	413.83
$C_{16}H_{14}CoN_6O_6$						
$[NiL\ (H_2O)_3]MeOH$	Dark yellow/8	80	42.80/42.65	3.80/3.81		
$C_{17}H_{18}NiN_6O_7$						
$[CuL\ H_2O]$	Olive/6.53	80	46.44/46.88	2.44/2.53		
$C_{16}H_{10}CuN_6O_4$						

All the synthesized complexes decompose without melting above 300 °C.

^a Λ_m /Molar conductance/ $\Omega^{-1}\ cm^2\ mol^{-1}$ molecular weight from mass spectrum.^b Calculated from TGA.**Table 2**IR spectral data (cm^{-1}) of the ligand (H_2L) and its complexes.

Compounds	ν_{OH}	$\nu_{C=N}$	ν_{NO_2}	$\nu_{N=N}$	ν_{C-O}	ν_{M-O}	ν_{M-N}
H_2L	3458	1633 1600 (sh)	1506	1419	1321	—	—
Cr(III)	3442	1634 1597	1502	1461	1282	549	439
Mn(II)	3430	1639 1604	1502	1463	1303	567	459
Co(II)	3442	1639 1604	1507	1464	1286	576	450
Ni(II)	3442	1638 1606	1509	1464	1291	567	460
Cu(II)	3444	1634 1600	1500	1465	1343	577	453

appeared within the ranges 273–500 and 318–444 °C for the Mn(II) and Cu(II) complexes, respectively, from which the organic ligand underwent decomposition leaving the ($MnO+2C$) and CuO as final product. For Co(II) and Ni(II) complexes, the thermal decomposition occurred within three successive steps. The first one within the ranges, 26–85 and 26–58 °C for Co(II) and Ni(II) complexes, respectively, can be attributed to the loss of lattice methanol or water molecule. The second step of decomposition appeared

within the ranges 85–120 and 58–100 °C for Co(II) and Ni(II) complexes, respectively, assigned to the loss of coordinated water. The organic ligand decomposed within the third step of decomposition which appeared within the ranges 336–390 and 378–414 °C for Co(II) and Ni(II) complexes, respectively, corresponding to the decomposition of the organic moiety with the formation of metal oxide as final product. For Co(II) complex, the last peak appeared as a sharp peak.

The kinetic parameters (of activation energy E, reaction order and Arrhenius pre-exponential factor A) for the final decomposition step were calculated using three mechanistic equations suggested by Coats-Redfern [44], Madhusudanan et. Al [45], and Wanjun et al. [46], at different heating rates (5–15 °C/min). The calculated various kinetic parameters are given in Tables 4–6. Three methods gave similar results.

The mechanism for the solid state thermal decomposition for the final decomposition stage in all the complexes was enunciated using the reported three mechanistic equations [44–46]. The selection of the mechanism which best describes the thermal decomposition of the complexes (Tables S1–S3) was calculated. The assignment of the mechanism is based on the assumption that the form of $g(\alpha)$ depends on the reaction mechanism. In the present investigations different forms of $g(\alpha)$ suggested by Satava [47], Table S4 was used to enunciate the mechanism of thermal

Table 3Thermogravimetric analysis data of the ligand (H_2L) and its metal complexes.

Compound	Temp. Range/°C	Mass loss/%		Assignment
		Found	Calc.	
H_2L	25–127	—	—	Thermal stable
	127–247	91.17	92.9	Loss of $C_{14}H_{10}N_6O_3$ from the organic ligand
	247–600	8.83	7.1	Complete decomposition of organic ligand
Cr(III)	29–100	5.90	6.82	Loss of coordinated methanol molecule
	100–179	3.18	4.11	Loss of coordinated water molecule
	179–267	7.72	8.46	Loss of coordinated chloride ion.
	312–400	63.28	63.50	Dissociation of the organic ligand with formation of Cr_2O_3 as final products
Mn(II)	26–142	4.49	4.44	Loss of coordinated water molecule
	273–500	71.51	72.12	Dissociation of the organic ligand with formation of $MnO + 4C$ as final products
Co(II)	26–85	7.98	8.42	Loss of lattice water molecules
	85–120	4.82	4.21	Loss of coordinated water molecule
	336–390	71.20	70.83	Dissociation of the organic ligand with formation of CoO as final products.
Ni(II)	26–58	6.28	6.70	Loss of lattice methanol molecule
	58–100	9.98	11.32	Loss of coordinated water molecules
	378–414	66.56	66.35	Dissociation of the organic ligand with formation of NiO as final product
Cu(II)	28–176	4.00	4.35	Loss of coordinated water molecule
	318–444	77.06	76.44	Dissociation of the organic ligand with formation of CuO as final product

Table 4

The kinetic and activation parameters (ΔH^* , ΔS^* , ΔG^*) for decomposition of the ligand and its complexes using Madhusudanan method [45].

Comp.	Heating rate	Model	R	A	E*	ΔH^*	$-\Delta S^*$	ΔG^*
Ligand Cr(III)	10	-ln (1- α)	0.9755	1305.9	81.12	76.98	0.1895	171.4
	5	-ln (1- α)	0.9976	2.97E+33	463.5	458.1	0.390	709.3
	10	-ln (1- α)	0.8854	1.5E+34	473.5	468.2	0.403	726.8
	15	-ln (1- α)	0.9994	2.0E+19	298.6	293.2	0.118	370.6
Mn(II)	5	-ln (1- α)	0.9977	78346	111.4	106.1	0.177	219.7
	10	-ln (1- α)	0.9855	3E+14	234.1	228.9	0.032	249.1
	15	-ln (1- α)	0.9530	7.8E+24	369.9	364.4	0.225	513.3
	5	-ln (1- α)	0.9921	3.98E+18	294.9	289.4	0.105	358.7
Co(II) Ni(II)	5	-ln (1- α)	0.9815	4.4E+56	529.5	523.8	0.450	828.5
	10	-ln (1- α)	0.9892	1.1E+33	495.7	489.9	0.38	753.7
	15	-ln (1- α)	0.9971	7.2E+26	409.5	403.8	0.262	583.7
	5	-ln (1- α)	0.9975	8.4E+22	342.2	336.8	0.187	459.2
Cu(II)	10	-ln (1- α)	0.9752	3.5E+57	777.5	772.0	0.850	1332.7
	15	-ln (1- α)	0.9950	1.67E+23	350.9	345.4	0.193	473.2

Where ΔH^* is the activation enthalpy (KJmol^{-1}), ΔS^* is the activation entropy ($\text{Jmol}^{-1}\text{K}^{-1}$), ΔG^* is the Gibbs activation free energy (KJmol^{-1}), h is the Plank constant, K_B is the Boltzmann constant and T is the observed peak temperature, universal gas constant,A the pre-exponential factor (s^{-1}).

Table 5

The kinetic and activation parameters (ΔH^* , ΔS^* , ΔG^*) for decomposition of the ligand and its complexes using Coats- Redfern method [44].

Complex	Heating rate	model	R	A	E*	ΔH^*	$-\Delta S^*$	ΔG^*
Ligand Cr(III)	10	-ln (1- α)	0.9753	581.7	79.1	74.99	0.196	171.7
	5	-ln (1- α)	0.9976	1.64E+33	463.0	457.7	0.385	705.7
	10	-ln (1- α)	0.8976	5.1E+36	475.2	469.9	0.401	727.6
	15	-ln (1- α)	0.9995	1.29E+19	298.9	293.5	0.114	368.4
Mn(II)	5	-ln (1- α)	0.9977	4297	110.99	105.6	0.182	222.8
	10	-ln (1- α)	0.9855	3.49E+14	233.6	228.4	0.027	245.5
	15	-ln (1- α)	0.9529	4.3E+24	369.4	363.9	0.220	509.6
	5	-ln (1- α)	0.9920	2.19E+18	294.5	288.99	0.095	354.97
Co(II) Ni(II)	5	-ln (1- α)	0.9815	2.43E+36	529	523	0.445	824.6
	10	-ln (1- α)	0.9893	5.81E+32	495.2	489.5	0.375	749.7
	15	-ln (1- α)	0.9973	3.98E+26	408.99	403.3	0.257	579.8
	5	-ln (1- α)	0.9975	4.6E+22	341.8	336.4	0.182	455.5
Cu(II)	10	-ln (1- α)	0.9759	2.2E+57	777.8	772.3	0.846	1330.4
	15	-ln (1- α)	0.9950	9.2E+22	350.5	344.9	0.188	469.4

Where ΔH^* is the activation enthalpy (KJmol^{-1}), ΔS^* is the activation entropy ($\text{Jmol}^{-1}\text{K}^{-1}$), ΔG^* is the Gibbs activation free energy (KJmol^{-1}), h is the Plank constant, K_B is the Boltzmann constant and T is the observed peak temperature, universal gas constant,A the pre-exponential factor (s^{-1}).

Table 6

The kinetic and activation parameters (ΔH^* , ΔS^* , ΔG^*) for decomposition of the ligand and its complexes using Wanjun method [46].

Complex	Heating rate	Model	r	A	E*	ΔH^*	$-\Delta S^*$	ΔG^*
Ligand Cr(III)	10	-ln (1- α)	0.9756	1256.2	79.5	78.43	0.190	168.98
	5	-ln (1- α)	0.9976	3.6E+33	463.7	458.3	0.391	710.5
	10	-ln (1- α)	0.8865	2.7E+34	475.8	470.4	0.408	732.4
	15	-ln (1- α)	0.9995	2.9E+19	299.5	294.1	0.121	373.3
Mn(II)	5	-ln (1- α)	0.9977	9563.8	111.6	106.2	0.175	218.8
	10	-ln (1- α)	0.9856	7.7E+14	234.2	228.9	0.034	250.2
	15	-ln (1- α)	0.9530	9.5E+24	370.0	364.5	0.227	514.5
	5	-ln (1- α)	0.9921	4.84E+18	295.1	289.6	0.106	359.9
Co(II) Ni(II)	5	-ln (1- α)	0.9815	5.4E+36	529.6	523.9	0.451	829.7
	10	-ln (1- α)	0.9892	1.29E+33	495.9	490.1	0.382	757.9
	15	-ln (1- α)	0.9971	8.8E+26	409.6	403.9	0.264	585.0
	5	-ln (1- α)	0.9975	1.02E+23	342.4	336.9	0.189	460.4
Cu(II)	10	-ln (1- α)	0.9759	4.8E+57	779.3	772.8	0.853	1335.3
	15	-ln (1- α)	0.9950	2E+23	351.1	345.6	0.195	474.4

Where ΔH^* is the activation enthalpy (KJmol^{-1}), ΔS^* is the activation entropy ($\text{Jmol}^{-1}\text{K}^{-1}$), ΔG^* is the Gibbs activation free energy (KJmol^{-1}), h is the Plank constant, K_B is the Boltzmann constant and T is the observed peak temperature, universal gas constant,A the pre-exponential factor (s^{-1}).

decomposition in each stage of complex. The correlation coefficients for all these nine forms were calculated and the form of $g(\alpha)$ for which the correlation has a maximum value was chosen as the mechanism of reaction. In the present investigation the highest value of correlation coefficient is obtained for $g(\alpha) = -\ln (1-\alpha)$. Thus, the mechanism is random nucleation with one nucleus on each particle representing Mampel model.

The thermodynamic parameters of activation (ΔH^* , ΔS^* and

ΔG^*) were estimated according to the previous methods with the aid of the following expressions:

$$\Delta H^* = E - RT$$

$$\Delta S^* = R \ln (hA/K_B T)$$

$$\Delta G^* = \Delta H^* - T\Delta S^*$$

where ΔH^* is the activation enthalpy (kJ mol^{-1}), ΔS^* is the activation entropy ($\text{J mol}^{-1}\text{K}^{-1}$), ΔG^* is the Gibbs activation free energy (kJ mol^{-1}), h is the Plank constant, K_B is the Boltzmann constant and T is the observed peak temperature, universal gas constant, A the pre-exponential factor (s^{-1})

According to the data obtained, the following remarks can be pointed out:

- 1 The high values of the energy of activation of the complexes (ΔE^*) reflect the high stability of the investigating complexes due to their covalent character [48].
- 2 For Co(II) complex, the kinetic and thermodynamic parameters increase with increasing the heating rate. For Cu(II) complex, these values decrease with increasing the heating rate. For the other complexes, the results show that the calculated values are independent on the heating rate.
- 3 The positive sign of ΔG^* for the complexes under investigation revealed that the free energy of the final residue is higher than that of the initial compound and all the decomposition steps are non-spontaneous processes [49,50].
- 4 The negative values of ΔS^* indicated a more order activated complex than reactant and/or the reaction was slow [51].
- 5 The positive values of ΔH^* means that the decomposition processes were endothermic [52].
- 6 The values of the kinetic parameters obtained by the three mentioned methods are in good agreement.

3.2.3. Electronic absorption and magnetic moment measurements

As the result of failure to obtain a single crystal for x-ray analyses, the electronic and magnetic measurements can be used to confirm the geometry of the investigated complexes.

The electronic absorption spectrum of Cr(III) complex displayed two bands at $14290, 18180\text{ cm}^{-1}$ due to the ${}^4A_2(\text{F}) \rightarrow {}^4T_1(\text{F})$ and ${}^4A_2(\text{F}) \rightarrow {}^4T_1(\text{p})$ transitions, respectively. This indicates the octahedral configuration around Cr(III) ion which was further deduced from the μ_{eff} value (4.02 BM) [53]. Mn(II) complex exhibited two bands at 19607 and 17857 cm^{-1} assigned as ${}^6A_1g \rightarrow {}^4T_1g$ and ${}^6A_1g \rightarrow {}^4Eg$ transition, respectively, assuming the square planar geometry for this complex [54]. The μ_{eff} value of Mn(II) complex is 4.4 BM indicating the presence of 3 unpaired electrons. The higher value may be due to orbital contribution [55]. Co(II) complex showed two bands at 14492 and 19492 cm^{-1} which may be assigned to ${}^4A_2(\text{F}) \rightarrow {}^4T_1(\text{F})$ and ${}^4A_2(\text{F}) \rightarrow {}^4T_1(\text{p})$, respectively, assuming the tetrahedral geometry around the Co(II) ion. The μ_{eff} value (4.81 BM) of complex verified the geometry of Co(II) complex [53]. The Nujol mull spectrum of Ni(II) complex displayed two bands at 14285 and 19607 cm^{-1} due to the ${}^4A_2(\text{F}) \rightarrow {}^4T_1(\text{F})$ and ${}^4A_2(\text{F}) \rightarrow {}^4T_1(\text{p})$ transitions, respectively. This indicates the octahedral configuration around Ni(II) ion. The μ_{eff} value (3.25 BM) of Ni(II) complex lies in the normal range (2.9–3.3 BM) observed for octahedral Ni(II) complexes [56]. The spectrum of Cu(II) complex displayed a band at 15384 cm^{-1} (${}^2B_{1g} \rightarrow {}^2E_{1g}$ transition) assuming square planar geometry around the central Cu(II) ion. The value of the magnetic moment (1.84 BM) of this complex confirmed the square planar geometry [57,58]. This μ_{eff} value is a typical for Cu(II) complexes supporting the exclusion of any perceivable spin-spin coupling between unpaired electrons of the various molecules [22,59].

The ligand field parameter B (interelectronic repulsion of the d electrons in complex), β (The Nephelauxetic effect) and $10Dq$ for Ni(II) complex are calculated according to the equations [60].

$$\mu_{\text{eff}} = \text{spin only}(1 - \alpha\lambda/10Dq)$$

$$B = \left[4(v_3 - 15Dq)^2 - 10Dq^2 \right] / [60(v_3 - 15Dq) - 180Dq]$$

$$v_1 = 10 Dq$$

$$\beta = B(\text{complex})/B(\text{free ion})$$

For Co(II), B (free ion) is 963 cm^{-1} and α is 4. The $10Dq$, B and β values are $2983, 614\text{ cm}^{-1}$ and 0.63, respectively. These results show that the interelectronic repulsion of the d electrons in a complex is less than in the free ion. The value of B in a Co(II) complex is 63% of the free-ion value. The β value is related directly to covalence, the reduction of B by complex formation is caused by delocalization of the d-electron.

Cloud on the ligand, which is in turn caused by the formation of covalent bond. The data show the Co(II) complex has covalent character [61].

The ligand field parameter B (interelectronic repulsion of the d electrons in complex), β (The Nephelauxetic effect) and $10Dq$ for Ni(II) complex are calculated according to the equations [62].

$$340Dq^2 - 18(v_2 + v_3)Dq + v_2v_3 = 0$$

$$B = \frac{v_2 + v_3 - 30Dq}{15}$$

where B (free ion) for Ni(II) is 1041 cm^{-1} . The $10Dq$ and B are 4256 and 739 cm^{-1} respectively and β value is 0.76. These results show that the interelectronic repulsion of the d electrons in a complex is less than in the free ion. The value of B in a complex is 70% of the free-ion value. The data show the Ni(II) complex has covalent character.

Based on the data of IR, UV–Vis spectra and magnetic moment values as well as the conductance values together with the data of elemental analysis, ICP and thermal analyses, the complexes can be formulated as follows:

3.2.4. Molecular modeling

Since our trials to obtain a single crystals of the metal complexes were unsuccessful so far, and in order to gain a better understanding of geometrical structures of the investigated complexes, molecular modeling studies have been done by means of Hyperchem program package. The molecular modeling of the ligand and all complexes were carried out for the proposed structures are given in Figs. 2–7. These values are obtained as a result of minimization of energy through MM2 method in Chem 3D Ultra 8.0.7. Some selected bond lengths of ligand and its complexes are listed in Table 7. The cis angles around Cr(III) ion are 92.95, 62.63, 90.26 and 137.00° but the trans angle is 136.06° . The values of bond angle confirmed the octahedral geometry around the Cr(III) ion. For Mn(II) and Cu(II) complexes, the copper and manganese atoms are situated almost exactly on the average plane defined by the donor atoms of the ligand and water molecule. The cis angles around the Mn(II) and Cu(II) ions in the range $86\text{--}98^\circ$ and $84\text{--}94^\circ$ for Mn(II) and Cu(II) complexes, respectively; the trans angles ranging from 159 to 174° and from 173 to 170° for Mn(II) and Cu(II) complexes, respectively, indicating square planar geometry with almost no tetrahedral distortion. For Co(II) complex, the angles around the Co(II) ion are 116.63, 116.23, 110.63 and 116.47° indicating tetrahedral geometry. For Ni(II) complex, the cis angle around Ni(II) ion are 104.60, 76.06, 76.72 and 103.70° but the trans angle is 160.95° . The values of the bond angle confirmed the octahedral geometry

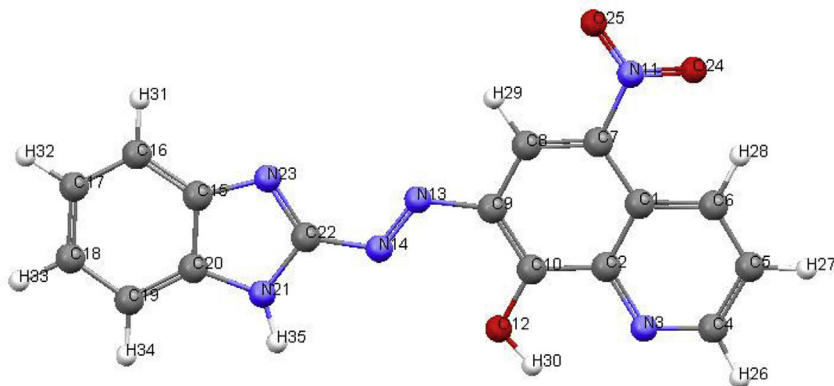


Fig. 2. Computational structure of the free azocompound, H_2L .

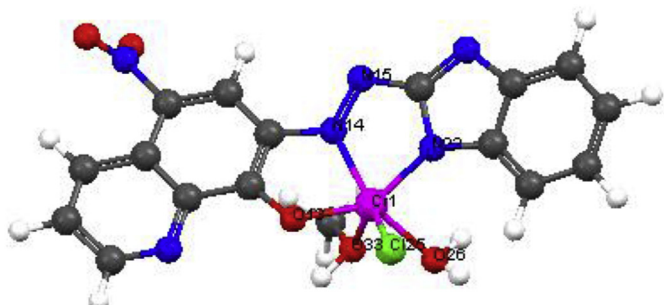


Fig. 3. Computational structure of $Cr^{(III)}$ complex.

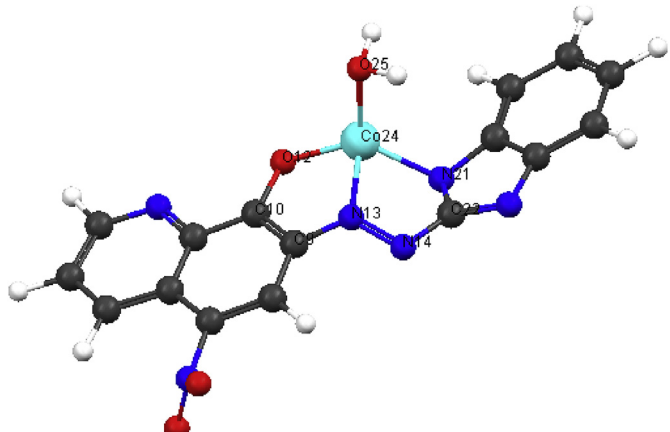


Fig. 5. Computational structure of $Co^{(II)}$ complex.

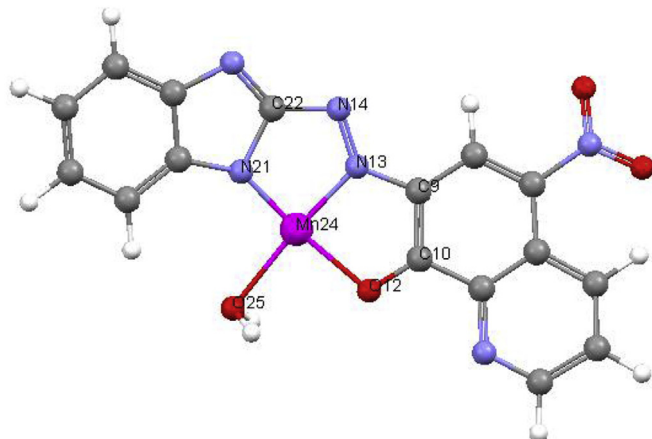


Fig. 4. Computational structure of $Mn^{(II)}$ complex.

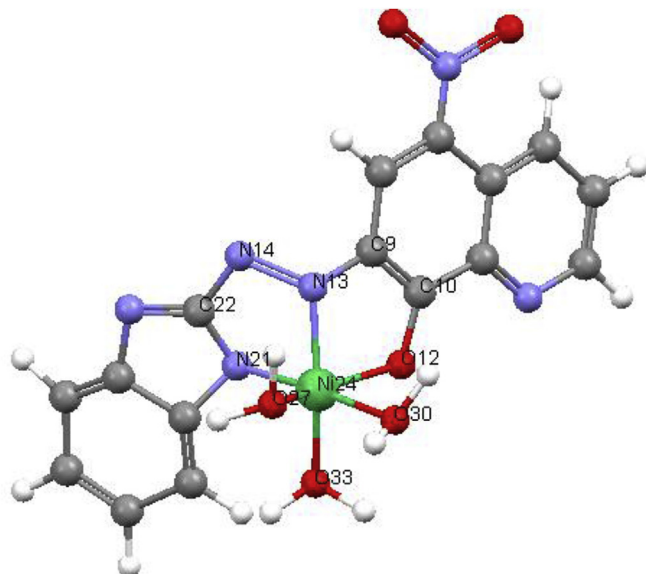


Fig. 6. Computational structure of $Ni^{(II)}$ complex.

around the $Ni^{(II)}$ ion. The obtained bond lengths of the $N=N$, $C-NH$ and $C-OH$ groups for the azodye ligand (H_2L) are 1.2338, 1.4134 and 1.3473\AA^0 , respectively. Based on the values in Table 7, it is observed that when the ligand is coordinated with the metal ions there is an change in the bond length in between the above mentioned atoms which confirms the coordination of azo, imino groups through nitrogen and deprotonated $C-OH$ through oxygen with all the metal ions. When the atoms are coordinated with the metal ion by donating a lone pair of electrons there is decrease of electron density on the coordinating atoms, hence bond length changes in metal complexes.

Quantum chemical parameters of compounds such as the energy of the highest occupied molecular orbital, E_{HOMO} , energy of the

lowest unoccupied molecular orbital, E_{LUMO} , energy gap (ΔE), electronegativity (χ), chemical potentials (P_i), dipole moment (μ), hardness (η), softness (σ), additional electronic charge (ΔN_{max})

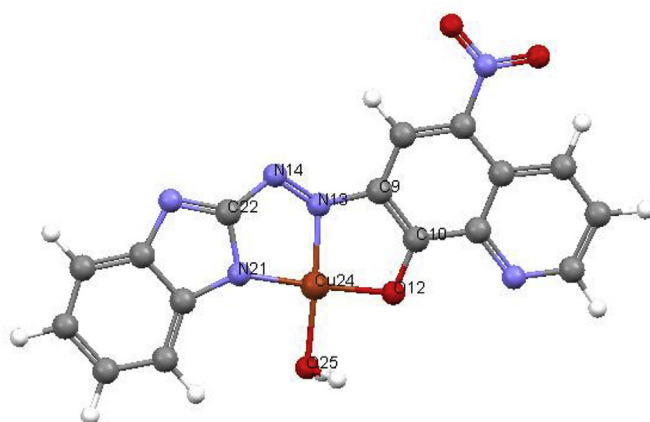


Fig. 7. Computational structure of Cu(II)complex.

have been calculated according to the equations in the literature [63]. The calculated data are listed in Table 8.

3.2.5. Antimicrobial activity

The biological activities of the synthesized compounds were screened for their antifungal activity (*C. albicans* and *A. niger*) and antibacterial activity (*E. coli* and *S. aureus*). The standard drugs, Fluconazole (antifungal) and Penicillin (antibacterial), were also tested at the same experimental conditions. The values of the diameter inhibition zone (mm) are listed in Table 9. The data listed

Table 9
The Inhibition zone diameter of the ligand (H_2L) and its complexes.

Compound	Inhibition zone diameter/mm			
	<i>C. albicans</i>	<i>A. niger</i>	<i>E. coli</i>	<i>S. aureus</i>
H_2L	9	9	10	11
Mn(II)	9	9	10	11
Co(II)	13	12	14	16
Ni(II)	12	13	16	14
Cu(II)	14	14	15	15
Fluconazole (antifungal)	24	21	—	—
Penicillin (antibacterial)	—	—	26	18

in Table 9 indicated that the Mn(II), Co(II), Ni(II) and Cu(II) complexes are good active than free ligand but less active than standard drugs. Co(II), Ni(II) and Cu(II) complexes have a good activity on *S. aureus*. Mn(II), Co(II), Ni(II) and Cu(II) complexes have moderate activity against *C. albicans* and *A. niger*. The Cu(II) complex has higher and the same activity on the two fungi organisms. The biological activity of the investigated azodye arises from the OH group which has an important role in the antimicrobial activity [64]. Upon complexation, the observed increased activity is due to fact that the positive charge of the metal ion is partially shared with the donor atoms of the ligand due to the electron delocalization over the whole chelating ring leading to the increased of the lipophilic character of the metal atom [65]. This favors its permeation more efficiently through the lipid layer of the microorganism, thus destroying them more aggressively. The ligand, Mn(II) and Co(II) complexes are more active against Gram + ve than Gram - ve bacteria leading the fact that the antibacterial activity of these

Table 7
Calculated bond lengths (Å) of the free ligand and its complexes.

compound	N=N	C–NH	C–OH	(N=N)–C (quinoline)	(N=N)–C (benzimidazole)	M–Cl	M–N	M–O
H_2L	1.2338	1.4134	1.3473	1.4369	1.4276	—	—	—
Cr(III)	1.3139	1.5160	1.3981	1.4431	1.3908	2.1667	1.9496 1.3908	1.8997 1.9893 2.0069
Mn(II)	1.2949	1.4998	1.2806	1.4043	1.4273	—	1.8498 1.7334	2.0417 2.1712
Co(II)	1.2544	1.3567	1.3758	1.2677	1.2729	—	1.8120 1.8200	1.7734 1.8204
Ni(II)	1.4800	1.3392	1.3827	1.3205	1.3706	—	1.8899 1.9307	1.8782 1.8693 1.8870 1.9047
Cu(II)	1.3482	1.4397	1.3479	1.4250	1.3821	—	1.8579 1.8662	1.8337 1.8902

Table 8
The theoretical parameters of molecular modeling of the ligand and its complexes.

Assignment of theoretical parameters	ligand	Cr(III)	Mn(II)	Co(II)	Ni(II)	Cu(II)
Total energy /kcal/mol	-89904	-103053	-105697	-114885	-135809	-124047
Binding energy /kcal/mol	-4022	-4266	-4253	-3499	-4906	-4285
Electronic energy	-635628	-777867	-788671	-8170371	-1046421	-849296
Heat of formation/kcal/mol	89	-30	-14	-125	-304	-33
Dipole moment/Debye	2.092	11.93	8.425	7.15	10.96	11.52
E_{LOMO} /eV	-1.49	-1.56	-2.04	-2.38	-0.76	-1.54
E_{HOMO} /eV	-9.06	-8.60	-9.19	-8.89	-8.45	-8.66
ΔE	7.57	7.04	7.15	6.51	7.69	7.12
χ	5.27	5.08	5.66	5.28	4.60	5.1
η	3.78	3.52	3.57	3.17	3.84	3.66
σ	0.26455	0.284091	0.280112	0.315457	0.260417	0.273224
Pi	-5.27	-5.08	-5.66	-5.28	-4.60	-5.1
ΔN_{max}	1.39418	1.443182	1.585434	1.665615	1.197917	1.393443

compounds is related to the cell wall structure of the bacteria.

3.2.6. Solid electrical conductivity studies

Electrical conduction of 7-((1H-benzo [d]imidazol-2-yl)diazaryl)-5-nitroquinolin-8-ol (H_2L) and its metal complexes was studied and described as a function of temperature from 298 to 525 K. Fig. 8 shows the temperature dependence of the AC resistivity, $\rho_{ac}(\omega)$, of the studied samples at different temperature. The values of AC resistivity indicate that the electrical conduction mechanism of the studied samples obeys the semiconducting band theory. It can be noted that at low frequency (1 kHz) the resistivity depends mainly on the contribution of the DC resistivity

component ρ_{dc} . The dispersive values of the AC resistivity was observed at 10 kHz where the resistivity obeys a power-law relation, $\rho(\omega) = \rho_{dc} + \beta \omega^n$ where β is temperature-dependent parameter, and n is a fractional exponent. It is observed that at high temperature region, the AC resistivity became frequency independent whereas it frequency dependent at low temperature and decreases by increasing frequency from 1 kHz to 10 kHz. Co(II), Ni(II) and Cu(II) complexes exhibited high electrical conductivities than Mn(II) complex and without doping complex. Partial oxidation of the copper-containing complex can result in the increase in the conductivity because at partial oxidation ratio the Columbic effects is not predominant leading to increase of the mobility. The thermal

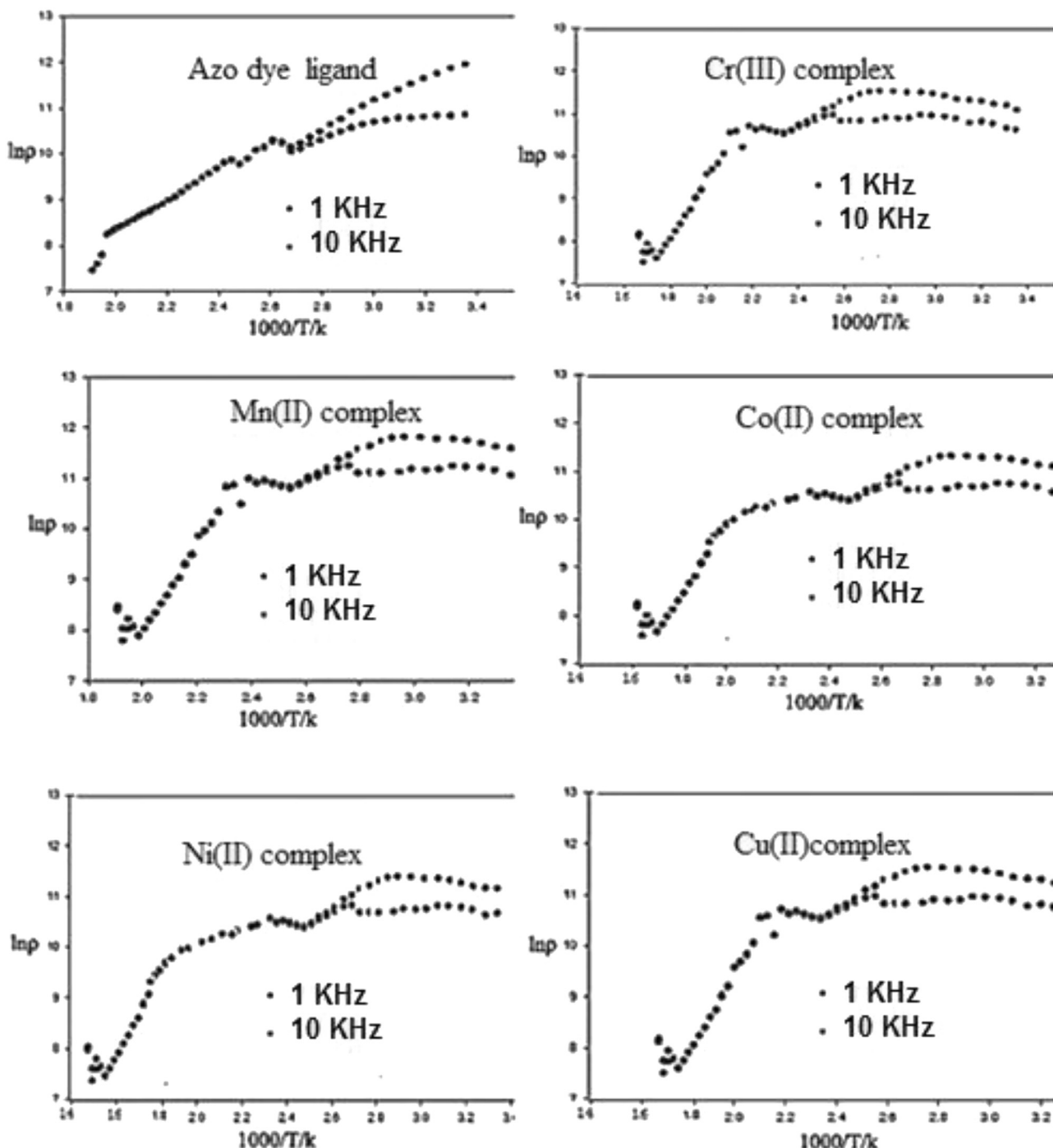


Fig. 8. AC resistivity as a function of temperature at two fixed frequencies 1KHz and 10 KHz.

properties of the metal complexes are discussed. The thermal activation energies of decomposition (E_a) of H_2L , Co(II), Ni(II) and Cu(II) complexes are 48.76, 30.59, 40.45 and 36.83 kJ/mol, respectively. Both of the ac conductivity and the values of the thermal activation energy for conduction, as well as the dielectric properties of the complexes of the azodye (H_2L) are found to depend on the nature of the metallic ions. The values of the activation energies of electrical conductivity decrease with increasing the value of applied frequency as given in Table 10. The AC resistivity results revealed that these complexes exhibit similar frequency dependent resistivity. The resistivity value ranging from 2.0 to 162 k Ω for the copper (II), nickel (II) and cobalt (II) complexes.

From these plots it is observed that all the samples show three regions with changing slope at different temperatures. It is suggested that the conduction mechanism changes from one region to another region. The conduction at low temperature <400 K obeys band theory, whereas at high temperature >400 K is due to polaron hopping. The calculated activation energies ΔE are greater than 0.4 eV which clearly suggest that the conduction is due to polar onhopping [66]. The activation energy calculated from resistivity curves are given Table 10. The behavior of activation energies with metal contents has the same trend as the variation of $(\ln \rho)$ vs. (metal content). This behavior of our results is similar to that in previous works [67,68]. Temperature dependence AC resistivity is related to the thermal activation of mobility of electric charge and follows Arrhenius relation:

$$\rho_1 = \rho_0 e^{E_a/K_p T}$$

where E_a is the activation energy for electric conduction and ρ_0 is the pre-exponential factor. The temperature T_c at the break point was calculated and tabulated in Table 10.

3.2.7. Temperature dependence of dielectric constant

The dielectric of the complexes has been studied using RLC bridge. The dielectric constant has been analyzed in the temperature range from 300 K to 520 K at constant frequencies 1 kHz and 10 kHz. A peak was observed for these set of complexes. The effect of temperature on the dielectric constant of the azo ligand is illustrated in Fig. 9. It is observed that the dielectric constant for the samples gradually increase with temperature up to 340 K. Above this temperature the dielectric constant sharply decreases. The mechanism of the polarization process is similar to that of the conduction process [69,70]. A similar temperature variation of the dielectric constant has been reported earlier [71–73]. The results also show that the dielectric constant ϵ decreases with increasing of the applied electric field frequency at low temperature. The value of T_c obtained from dielectric measurement is nearly equal to that obtained from resistivity measurement. At low temperatures the dielectric constant increases by increasing temperature due to the increase of electric space charge polarization. Above T_c , the change in conduction mechanism decrease the polarization and hence decrease the dielectric constant. At high frequency 10 kHz, the charge carriers cannot follow the variation of the external electric field leading to the decrease of conductivity and the dielectric constant.

Table 10

The values of the activation energies of electrical conductivity of the azodye and its metal complexes.

Compound	H_2L	Cr(II) Complex	Mn(II) complex	Co(II) complex	Ni(II) Complex	Cu(II) Complex
$E/eV/1\text{ kHz}$	0.735	0.608	0.606	0.566	0.506	0.466
$E/eV/10\text{ kHz}$	0.706	0.599	0.593	0.536	0.496	0.406
T_c	384	454	416	420	400	384

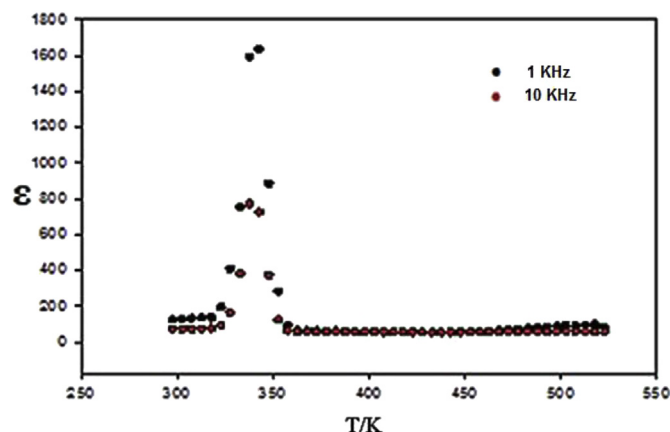


Fig. 9. The effect of temperature on the dielectric constant of the azo ligand.

4. Conclusion

In this study, a new azo-compound -((1H-benzo [d]imidazol-2-yl) diazenyl)-5-nitroquinolin-8-ol, and its Cr(III), Mn(II), Co(II), Ni(II) and Cu(II) complexes have synthesized. The structure and geometry of the isolated complexes have been identified and confirmed by elemental analyses, spectral studies (mass spectra, IR, electronic, ESR) and magnetic data as well as the thermal studies. The IR spectral data supported the involvement of nitrogen atom of azo-group and deprotonated OH and NH groups in complex formation indicating that the titled azo ligand acts as dibasic tridentate ligand with NNO sites. The present study revealed the octahedral geometry around Cr (III) and Ni(II) complexes; tetrahedral for Co(II) complex and square planar for Mn(II) and Cu(II) complexes. The thermal decomposition of the metal complexes was studied by TGA technique from which the kinetic and thermodynamic parameters of the thermal decomposition of the complexes have been evaluated using three mechanistic equations at different heating rates (5–15 °C/min). The values of the kinetic parameters obtained by the three mentioned methods are in good agreement. The titled compoundshave also been screened for their antimicrobial and antifungal activities. The obtained data pointed out that the antimicrobial activity of the metal complexes are good active than ligand but less active than standarddrugs such as Fluconazole or Penicillin. The observed higher antibacterial activities of the metal complexes are due to the fact that these compounds are more susceptible towards the bacterial cell. The variation of the activity of the investigated compounds against different organisms depends either on ribosomes in microbial cells or on the impermeability of the cell of the microbes. The data indicated that the antimicrobial activity is related to the cell wall structure of the bacteria. The electrical conductance of the azodye and its metal complexes was measured at different temperatures (25–252 °C) using different frequency values. The results of conductance pointed out that the electrical conduction mechanism of the studied samples obeys the semiconducting band theory. The dielectric constant of the ligand has been analyzed in the temperature range from 300 K to 520 K at constant frequencies 1 KHZ and

10 KHZ. It is observed that the dielectric constant gradually increase with temperature up to 340 K then decreases. The mechanism of the polarization process is similar to that the conduction process. The results also show that the dielectric constant ϵ decreases with increasing the applied electric field frequency at low temperature.

Acknowledgements

Financial support from Tanta University, Tanta, Egypt is gratefully acknowledged.

Appendix A. Supplementary data

Supplementary data to this article can be found online at <https://doi.org/10.1016/j.molstruc.2018.12.006>.

References

- [1] H. Tian, X. Chang, Z. Hu, K. Yang, Q. He, L. Zhang, Z. Tu, Activated carbon modified with 4-(8-hydroxyquinoline-azo) benzamidine for selective solid phase extraction and preconcentration of trace lead from environmental samples, *Microchim. Acta* 171 (2010) 225–232.
- [2] K. El-Baradie, R. El-Sharkawy, H. El-Ghamry, K. Sakai, Synthesis and characterization of Cu(II), Co(II) and Ni(II) complexes of a number of sulfadiazoydyes and their application for wastewater treatment, *Spectrochim. Acta* 121 (2014) 180–187.
- [3] N.A. El-Ghamaz, A.Z. El-Sonbati, M.A. Diab, A.A. El-Binary, G.G. Mohamed, Sh Morgan, Correlation between ionic radii of metal azodye complexes and electrical conductivity, *Spectrochim. Acta* 147 (2015) 200–211.
- [4] A. Khedr, M. Gaber, R. Issa, H. Erten, Synthesis and spectral studies of 5-[3-(1,2,4-triazolylazo)-2,4-dihydroxy benzaldehyde (TA) and its Schiff bases with 1,3-diaminopropane (TAAP) and 1,6-diaminohexane (TAAH). Their analytical application for spectrophotometric microdetermination of Cobalt(II). Application in some radiochemical studies, *Dyes Pigments* 67 (2005) 117–126.
- [5] A. Khedr, M. Gaber, Spectrophotometric studies of the reaction of Zn(II) with some azotriazole compounds and its application to the spectrophotometric determination of micro- amount of Zn(II), *Spectrosc. Lett.* 38 (2005) 431–445.
- [6] Y. Cheng, M. Zhang, H. Yang, F. Li, T. Yi, C. Huang, Azo dyes based on 8-hydroxyquinoline benzoates: synthesis and application as colorimetric Hg^{2+} -selective chemosensors, *Dyes Pigments* 76 (2008) 775–783.
- [7] A. El-Sonbati, M. Diab, A. El-Binary, A. ElDesoky, M. Morgan, Correlation between ionic radii of metals and thermal decomposition of supramolecular structure of azodye complexes, *Spectrochim. Acta* 135 (2015) 774–779.
- [8] J. Griffiths, *Colour and Constitution of Organic Molecules*, Academic Press, New York and London, 1976, pp. 193–195.
- [9] G. Hussain, M. Ather, M. Ain Khan, A. Saeed, R. Saleem, G. Shabir, P. Channar, Synthesis and characterization of chromium (III), iron (II), copper (II) complexes of 4-amino-1-(p-sulphophenyl)-3-methyl-5-pyrazolonebased acid dyes and their applications on leather, *Dyes Pigments* 130 (2016) 90–98.
- [10] F. Karipcin, B. Dede, S. Percin-Ozkorucuklu, E. Kabalcil, Mn(II), Co(II) and Ni(II) complexes of 4-(2-thiazolylazo)resorcinol: syntheses, characterization, catalase-like activity, thermal and electrochemical behaviour, *Dyes Pigments* 84 (2009) 14–18.
- [11] K. Al-Adilee, A. Abass, A. Taher, Synthesis of some transition metal complexes with new heterocyclic thiazolylazo dye and their uses as sensitizers in photo reactions, *J. Mol. Struct.* 1108 (2016) 378–397.
- [12] K. Naresh Kumar, R. Ramesh, Yu Liu, Synthesis, structure and catalytic activity of cycloruthenated carbonyl complexes containing arylazophenolate ligands, *J. Mol. Catal. Chem.* 265 (2007) 218–226.
- [13] F. Gan, L. Hou, G. Wang, H. Liu, J. Li, Optical and recording properties of short wavelength optical storage materials, *Mater. Sci. Eng., B* 76 (2000) 63–68.
- [14] X.Y. Li, Y.Q. Wu, D.D. Gu, F.X. Gan, Optical characterization and blu-ray recording properties of metal(II) azobabarbituric acid complex films, *Mater. Sci. Eng., B* 158 (2009) 53–57.
- [15] H. Dinçalp, S. Yavuz, Ö. Hakki, C. Zafer, S. İçli, Optical and photovoltaic properties of salicylaldimine-based azo ligands, *J. Photochem. Photobiol. Chem.* 210 (2010) 8–16.
- [16] A. Khedr, M. Gaber, E. Abd El-Zaher, Synthesis, structural characterization and antimicrobialactivities of Mn(II),Co(II), Ni(II), Cu(II) and Zn(II) complexes of triazole based azodyes, *Chin. J. Chem.* 29 (2011), 1124–113.
- [17] M. Gaber, Y. El-Sayed, K. El-Baradie, R. Fahmy, Complex formation, thermal behavior and stability competition between Cu(II) ion and Cu⁰ nanoparticles with some new azodyes. Antioxidant and in vitro cytotoxic activity, *Spectrochim. Acta* 107 (2013) 359–370.
- [18] A. Khedr, M. Gaber, K. Saad-Ilah, Synthesis, characterization and antimicrobial efficiency of some Zirconyl(II) complexes involving O,N-Donor environment of Triazole based azodyes, *Chin. J. Inorg. Chem.* 30 (2014) 1201–1211.
- [19] A. Alaghaz, M. Zayed, S. Alharbi, Synthesis, spectral characterization, molecular modeling and antimicrobial studies of tridentate azo-dye Schiff base metal complexes, *J. Mol. Struct.* 1084 (2015) 36–45.
- [20] S.A. AbouEl-Enein, S.M. Emam, M.W. Polis, E.M. Emara, Synthesis and characterization of some metal complexes derived from azo compound of 4,4'-methyleneedianiline and antipyrine: evaluation of their biological activity on some land snail species, *J. Mol. Struct.* 1099 (2015) 567–578.
- [21] W. Mahmoud, M. Omar, F. Sayed, Synthesis, spectral characterization, thermal, anticancer and antimicrobial studies of bidentateazo dye metal complexes, *J. Therm. Anal. Calorim.* 124 (2016) 1071–1089.
- [22] H. El-Ghamry, S. Fathalla, M. Gaber, Synthesis, structural characterization and molecular modelling of bidentateazo dye metal complexes: DNA interaction to antimicrobial and anticancer activities, *Appl. Organomet. Chem.* (2018), <https://doi.org/10.1002/aoc.4136>.
- [23] M.A. Zayed, G.G. Mohamed, S.A.M. Abdulla, Synthesis,structure investigation, spectral characteristics and biological activities of some novel azodyes, *Spectrochim. Acta* 78 (2011) 1027–1036.
- [24] A.Z. El-Sonbati a, M.A. Diab, A.A. El-Binary, A.F. Shoair, M.A. Hussein, R.A. El-Boz, Spectroscopic, thermal, catalytic and biological studies of Cu(II) azodye complexes, *J. Mol. Struct.* 1141 (2017) 186–203.
- [25] B. Mahapatra, S. Chaulia, A. Sarangi, S. Dehury, J. Panda, Synthesis characterisation, spectral, thermal, XRD, molecular modelling and potential antibacterial study of metal complexes containing octadentateazodiyeligands, *J. Mol. Struct.* 1087 (2015) 11–25.
- [26] A. Alaghaz, M.E. Zayed, R.A.A. Ammar, A. Elhenawy, Synthesis, characterization, biological activity, molecular modeling and docking studies of complexes 4-(4-hydroxy)-3-(2-pyrazine-2-carbonyl)hydrazonomethylphenyl-dienaz-enylbenzenesulfonamide with manganese(II), cobalt(II), nickel(II), zinc(II) and cadmium(II), *J. Mol. Struct.* 1084 (2015) 352–362.
- [27] J. Xie, L. Fan, L. Su, H. Tian, Novel polymeric metal complexes based on bis (8-hydroxy quinolinol), *Dyes Pigments* 59 (2003) 153–162.
- [28] M. Hebrant, M. Rose-Helene, J.oly, A. Walcarius, Kinetics of the complexation of Ni²⁺ ions by 5-phenyl-azo-8-hydroxyquinoline grafted on colloidal silica particles, *Colloid. Surface. Physicochem. Eng. Aspects.* 380 (2011) 261–269.
- [29] A. Zidan, A. El-Said, M. El-Meligy, A. Aly, O. Mohammed, Mixed ligand complexes of 5-arylazo-8-hydroxyquinoline and α -amino acids with Co(II), Ni(II) and Cu(II), *J. Therm. Anal. Calorim.* 62 (2000) 665–679.
- [30] Y. Kovtun, Y. Prostota, A. Tolmachev, Metallechromicmerocyanines of 8-hydroxy quinoline series, *Dyes Pigments* 58 (2003) 83–91.
- [31] R. Lee, E. Griswold, J. Kleinberg, Studies on the stepwise controlled decomposition of 2,2'-bipyridine complexes of cobalt(II) and nickel(II) chlorides, *Inorg. Chem.* 3 (1964) 1278–1283.
- [32] P.W. Selwood, *Magnetochemistry*, Interscience Publisher, New York, 1956, p. 78.
- [33] HyperChem Version 8.0 Hypercube, Inc.
- [34] R. Cooper, F.W. Kavanagh, *Analytical Microbiology*, vols. 1 & 11, Academic press, New York & London, 1972.
- [35] W. Geary, The use of conductivity measurements in organic solvents for the characterization of coordination compounds, *Coord. Chem. Rev.* 7 (1971) 81–122.
- [36] A.M. Mansour, N.T. Abdel-Ghani, Synthesis, spectroscopic, DFT, cytotoxicity and antimicrobial activity of Pd(II) and Pt(II) complexes of N,N-chelated benzimidazole derivatives, *Inorg. Chim. Acta* 438 (2015) 76–84.
- [37] M. Gaber, G.B. El-Hefnawy, M.A. El-Borai, N.F. Mohamed, Synthesis spectral and thermal studies of Mn(II), Co(II), Ni(II), Cu(II) and Zn(II) complex dyes based on hydroxyquinoline moiety, *J. Therm. Anal. Calorim.* 109 (2012) 1397–1405.
- [38] S. Sarkar, K. Dey, Synthesis and spectroscopic characterization of some transition metal complexes of a new hexadentate $N_2S_2O_2$ Schiff base ligand, *Spectrochim. Acta* 62 (2005) 383–393.
- [39] N.H. Yarkandi, H.A. El-Ghamry, M. Gaber, Synthesis, spectroscopic and DNA binding ability of Co^{II}, Ni^{II}, Cu^{II} and Zn^{II} complexes of Schiff base ligand (E)-1(((1H-benzo[d]imidazol-2-yl) methylimino) methyl)naphthalen-2-ol. X-ray crystal structure determination of cobalt (II) complex, *Mater. Sci. Eng. C* 75 (2017) 1059–1067.
- [40] M.M. Omar, G.G. Mohamed, Potentiometric, spectroscopic and thermal studies on the metal chelates of 1-(2-thiazolylazo)-2-naphthalenol, *Spectrochim. Acta* 61 (2005) 929–936.
- [41] A. EL-Tabl, F.A. EL-Saeid, A. AL-Hakimi, Synthesis, spectroscopic investigation and biological activity of metal complexes with ONO tri function alized hydrazone ligand, *Transition Met. Chem.* 32 (2007) 689–701.
- [42] M. Tunçel, H. Kahyaoglu, M. Çakır, Synthesis, characterization, and histological activity of novel polydentate azo ligands and their cobalt(II), copper(II) and nickel(II) complexes, *Transition Met. Chem.* 3 (2008) 605–613.
- [43] K. Nakamoto, *Infrared and Raman Spectra of Inorganic and Coordination Compounds*, Wiley-Interscience, New York, 1986.
- [44] A. Coats, J. Redfern, Kinetic parameters from thermogravimetric data, *Nature* 201 (1964) 68–69.
- [45] P. Madhusudanan, K. Krishnan, K. Ninan, New equations for kinetic analysis of non-isothermal reactions, *Thermochim. Acta* 22 (1993) 13–21.
- [46] T. Wanju, L. Yuwen, Z. Hen, W. Cunxin, New temperature integral approximate formula for non-isothermal kinetic analysis, *J. Therm. Anal. Calorim.* 74 (2003) 309–315.
- [47] V. Satava, Mechanism and kinetics from non-isothermal thermogravimetric traces, *Thermochim. Acta* 2 (1971) 423–428.
- [48] T. Takeyama, F. Quinn, *Thermal Analysis Fundamentals and Applications to Polymer Science*, John Wiley and Sons, Chichester, 1994.

- [49] P. Maravalli, T. Goudar, Thermal and spectral studies of 3-N-methyl morpholino-4-amino-5-mercaptopro-1,2,4-triazole and 3-N-methyl-piperidino-4-amino-5-mercaptopro-1,2,4-triazole complexes of cobalt(II), nickel(II) and copper(II), *Thermochim. Acta* 235 (1999) 35–41.
- [50] N. Madhu, P. Radhakrishnan, E. Williams, W. Linert, Thermal decomposition studies on cobalt(II) complexes of 4-N-(4'-antipyrylmethylene)amino-antipyryne with varying counter ions, *J. Therm. Anal. Calorim.* 79 (2005) 157–161.
- [51] S. Matheu, C. Nair, K. Ninan, Thermal decomposition kinetics: Part XV. Kinetics and mechanism of thermal decomposition of tetramminecopper(II) sulphate monohydrate, *Thermochim. Acta* 144 (1989) 33–43. A. Frost, R. Pearson. *Kinetics and Mechanisms*, Wiley, New York, 1961.
- [52] M. Gaber, H. El-Ghamry, S. Fathalla, Ni(II), Pd(II) and Pt(II) complexes of (1H-1,2,4-triazole-3 ylimino) methyl naphthalene -2-ol Structural, spectroscopic, biological, cytotoxicity, antioxidant and DNA binding, *Spectrochim. Acta A* 139 (2015) 396–404.
- [53] M.S. Masoud, A.E. Ali, M.A. Shaker, G.S. Elasala, Synthesis, computational, spectroscopic, thermal and antimicrobial activity studies on some metal–urate complexes, *Spectrochim. Acta A* 90 (2012) 93–108.
- [54] J.C. Bailar, H.J. Emeleus, R. Nyholm, A.F. Trotman-Dickenson, *Comprehensive Inorganic Chemistry*, vol. 3, Pergamon Press, New York, 1975.
- [55] T. Al-Nahary, Synthesis and characterization of metal complexes of Cr(III), Mn(II), Fe(III), Co(II), Ni(II), Cu(II), Ru(III), Rh(III) and Pd(II) with derivatives of 1,3,4-thiadiazole-2,5-dithiol as new ligands, *J. Saudi Chem. Soc.* 13 (2009) 253–257.
- [56] A.M. Ali, A.H. Ahmed, T.A. Mohamed, B.H. Mohamed, Chelates and corrosion inhibition of newly synthesized Schiff bases derived from o-tolidine Transition, *Met. Chem.* 32 (2007) 461–467.
- [57] A. El-Asmy, A.Z. Al-Abdeen, W.M. Abo El-Maaty, M.M. Mostafa, Synthesis and spectroscopic studies of 2,5-hexanedione bis(isonicotinyl hydrazone) and its first raw transition metal complexes, *Spectrochim. Acta* 75 (2010) 1516–1522.
- [58] P. Sambasiva Reddy, K. Hussain Reddy, Transition metal complexes of benzil- α -monoxime (BMO): X-ray structure determination of Co(BMO)₃, *Polyhedron* 19 (2000) 1687–1692.
- [59] J.R. Gispert, *Coordination Chemistry*, Wiley-VCH, Weinheim, 2008.
- [60] O. Adly, Synthesis, molecular modeling, thermal and spectral studies of metal complexes of hydrazone derived from 5-acetyl-4-hydroxy-2H-1,3-thiazine-2,6(3H)-dione and thiosemicarbazide, *Spectrochim. Acta* 79 (2011) 1295–1303.
- [61] D. Nichlis, *Complexes and First-row Transition Elements*, 1974, p. 92 (Chapter 5).
- [62] C. Jorgensen, *Absorption Spectra and Chemical Bonding in Complexes*, Pergamon Press, London, 1962.
- [63] M. Aljahdali, A. El-Sherif, Synthesis, characterization, molecular modeling and biological activity of mixed ligand complexes of Cu(II), Ni(II) and Co(II) based on 1,10-phenanthroline and novel thiosemicarbazone, *Inorg. Chim. Acta* 407 (2013) 58–68.
- [64] A. Chaudhary, R. Singh, Synthetic, structural and biological studies on divalent tin complexes of sixteen to twenty-four membered TetraazaMacrocycles phosphorus, sulfur, Silicone Relat. Elem. 178 (2003) 603–613.
- [65] M. Ahmed, M. El-Nimr, M. Amer, The ac electrical conductivity for Co-substituted SbNi ferrites, *J. Magn. Magn Mater.* 152 (1996) 391–395.
- [66] M. Linger, Two-phase polaron model of conduction in magnetite-like solids, *J. Phys. C8* (1975) 3595.
- [67] K. Krishna, K. Kumar, D. Ravinder, Structural and electrical conductivity studies in nickel-zinc ferrite, *Adv.in Mat.Phys.and Chem.* 2 (2012) 185–191.
- [68] A. Verma, O. Thakur, C. Prakash, T. Goel, R. Mediratta, Temperature dependence of electrical properties of nickel-zinc ferrites processed by the citrate precursor technique, *Mat. Sci.Engin., B* 116 (2005) 1–6.
- [69] K. Iwaudri, Dielectric properties of fine particles of Fe₃O₄ and some ferrites, *Jpn. J. Appl. Phys.* 10 (1971) 1520.
- [70] L. Rabinkin, Z. Novikova, *Ferrites*. Minsk: Izv. Acad. Nauk USSR (1960) 146.
- [71] S. Olofa, Oscillographic study of the dielectric polarization of Cu-doped NiZn ferrite, *J. Magn. Magn. Mater.* 131 (1994) 103–106.
- [72] K. Yadav, R. Chowdhary, Structural and electrical properties of PZT (La, Na) ceramics, *Mater. Lett.* 19 (1994) 61–64.
- [73] S. Bera, R. Chowdhary, Structural, SEM and electrical properties of Pb(Li_{1/4}Y_{1/4}W_{1/2}O₃, *Mater. Lett.* 22 (1995) 197–201.